

Search for Dark Matter Particle Interactions with Electron Final States with DarkSide-50

P. Agnes,¹ I. F. M. Albuquerque,² T. Alexander,³ A. K. Alton,⁴ M. Ave,² H. O. Back,³ G. Batignani,^{5,6} K. Biery,⁷ V. Bocci,⁸ W. M. Bonivento,⁹ B. Bottino,^{10,11} S. Bussino,^{12,13} M. Cadeddu,⁹ M. Cadoni,^{14,9} F. Calaprice,¹⁵ A. Caminata,¹¹ M. D. Campos,¹⁶ N. Canci,¹⁷ M. Caravati,⁹ N. Cargioli,⁹ M. Cariello,¹¹ M. Carlini,^{17,18} V. Cataudella,^{19,20} P. Cavalcante,^{21,17} S. Cavanaugh,^{19,20} S. Chashin,²² A. Chepurinov,²² C. Cicalò,⁹ G. Covone,^{19,20} D. D'Angelo,^{23,24} S. Davini,¹¹ A. De Candia,^{19,20} S. De Cecco,^{8,25} G. De Filippis,^{19,20} G. De Rosa,^{19,20} A. V. Derbin,²⁶ A. Devoto,^{14,9} M. D'Incecco,¹⁷ C. Dionisi,^{8,25} F. Dordei,⁹ M. Downing,²⁷ D. D'Urso,^{28,29} G. Fiorillo,^{19,20} D. Franco,³⁰ F. Gabriele,⁹ C. Galbiati,^{15,18,17} C. Ghiano,¹⁷ C. Giganti,³¹ G. K. Giovanetti,¹⁵ A. M. Goretti,¹⁷ G. Grilli di Cortona,³² A. Grobov,^{33,34} M. Gromov,^{22,35} M. Guan,³⁶ M. Gulino,^{37,29} B. R. Hackett,³ K. Herberichs,⁷ T. Hessel,³⁰ B. Hosseini,⁹ F. Hubaut,³⁸ E. V. Hungerford,³⁹ An. Ianni,^{15,17} V. Ippolito,⁸ K. Keeter,⁴⁰ C. L. Kendziora,⁷ M. Kimura,⁴¹ I. Kochanek,¹⁷ D. Korabely,³⁵ G. Korga,^{39,17} A. Kubankin,⁴² M. Kuss,⁵ M. La Commara,^{19,20} M. Lai,^{14,9} X. Li,¹⁵ M. Lissia,⁹ G. Longo,^{19,20} O. Lychagina,^{35,22} I. N. Machulin,^{33,34} L. P. Mapelli,⁴³ S. M. Mari,^{12,13} J. Maricic,⁴⁴ A. Messina,^{8,25} R. Milincic,⁴⁴ J. Monroe,¹ M. Morrocchi,^{5,6} X. Mougeot,⁴⁵ V. N. Muratova,²⁶ P. Musico,¹¹ A. O. Nozdrina,^{33,34} A. Oleinik,⁴² F. Ortica,^{46,47} L. Pagani,⁴⁸ M. Pallavicini,^{10,11} L. Pandola,²⁹ E. Pantic,⁴⁸ E. Paoloni,^{5,6} K. Pelczar,^{17,49} N. Pelliccia,^{46,47} S. Piacentini,⁸ A. Pocar,²⁷ D. M. Poehlmann,⁴⁸ S. Pordes,⁷ S. S. Poudel,³⁹ P. Pralavorio,³⁸ D. D. Price,⁵⁰ F. Ragusa,^{23,24} M. Razeti,⁹ A. Razeto,¹⁷ A. L. Renshaw,³⁹ M. Rescigno,⁸ J. Rode,^{31,30} A. Romani,^{46,47} D. Sablone,^{15,17} O. Samoylov,³⁵ W. Sands,¹⁵ S. Sanfilippo,^{13,12} E. Sandford,⁵⁰ C. Savarese,¹⁵ B. Schlitzer,⁴⁸ D. A. Semenov,²⁶ A. Shchagin,⁴² A. Sheshukov,³⁵ M. D. Skorokhvatov,^{33,34} O. Smirnov,³⁵ A. Sotnikov,³⁵ S. Stracka,⁵ Y. Suvorov,^{19,20,33} R. Tartaglia,¹⁷ G. Testera,¹¹ A. Tonazzo,³⁰ E. V. Unzhakov,²⁶ A. Vishneva,³⁵ R. B. Vogelaar,²¹ M. Wada,^{41,14} H. Wang,⁴³ Y. Wang,^{43,36} S. Westerdale,^{15,9} M. M. Wojcik,⁴⁹ X. Xiao,⁴³ C. Yang,³⁶ and G. Zuzel⁴⁹

(DarkSide Collaboration)

¹*Department of Physics, Royal Holloway University of London, Egham TW20 0EX, United Kingdom*²*Instituto de Física, Universidade de São Paulo, São Paulo 05508-090, Brazil*³*Pacific Northwest National Laboratory, Richland, Washington 99352, USA*⁴*Physics Department, Augustana University, Sioux Falls, South Dakota 57197, USA*⁵*INFN Pisa, Pisa 56127, Italy*⁶*Physics Department, Università degli Studi di Pisa, Pisa 56127, Italy*⁷*Fermi National Accelerator Laboratory, Batavia, Illinois 60510, USA*⁸*INFN Sezione di Roma, Roma 00185, Italy*⁹*INFN Cagliari, Cagliari 09042, Italy*¹⁰*Physics Department, Università degli Studi di Genova, Genova 16146, Italy*¹¹*INFN Genova, Genova 16146, Italy*¹²*INFN Roma Tre, Roma 00146, Italy*¹³*Mathematics and Physics Department, Università degli Studi Roma Tre, Roma 00146, Italy*¹⁴*Physics Department, Università degli Studi di Cagliari, Cagliari 09042, Italy*¹⁵*Physics Department, Princeton University, Princeton, New Jersey 08544, USA*¹⁶*Physics, Kings College London, Strand, London WC2R 2LS, United Kingdom*¹⁷*INFN Laboratori Nazionali del Gran Sasso, Assergi (AQ) 67100, Italy*¹⁸*Gran Sasso Science Institute, L'Aquila 67100, Italy*¹⁹*Physics Department, Università degli Studi "Federico II" di Napoli, Napoli 80126, Italy*²⁰*INFN Napoli, Napoli 80126, Italy*²¹*Virginia Tech, Blacksburg, Virginia 24061, USA*²²*Skobeltsyn Institute of Nuclear Physics, Lomonosov Moscow State University, Moscow 119234, Russia*²³*Physics Department, Università degli Studi di Milano, Milano 20133, Italy*²⁴*INFN Milano, Milano 20133, Italy*²⁵*Physics Department, Sapienza Università di Roma, Roma 00185, Italy*²⁶*Saint Petersburg Nuclear Physics Institute, Gatchina 188350, Russia*²⁷*Amherst Center for Fundamental Interactions and Physics Department, University of Massachusetts, Amherst, Massachusetts 01003, USA*²⁸*Chemistry and Pharmacy Department, Università degli Studi di Sassari, Sassari 07100, Italy*²⁹*INFN Laboratori Nazionali del Sud, Catania 95123, Italy*

- ³⁰*APC, Université de Paris, CNRS, Astroparticule et Cosmologie, Paris F-75013, France*
³¹*LPNHE, CNRS/IN2P3, Sorbonne Université, Université Paris Diderot, Paris 75252, France*
³²*INFN Laboratori Nazionali di Frascati, Frascati 00044, Italy*
³³*National Research Centre Kurchatov Institute, Moscow 123182, Russia*
³⁴*National Research Nuclear University MEPhI, Moscow 115409, Russia*
³⁵*Joint Institute for Nuclear Research, Dubna 141980, Russia*
³⁶*Institute of High Energy Physics, Beijing 100049, China*
³⁷*Engineering and Architecture Faculty, Università di Enna Kore, Enna 94100, Italy*
³⁸*Centre de Physique des Particules de Marseille, Aix Marseille Univ, CNRS/IN2P3, CPPM, Marseille, France*
³⁹*Department of Physics, University of Houston, Houston, Texas 77204, USA*
⁴⁰*School of Natural Sciences, Black Hills State University, Spearfish, South Dakota 57799, USA*
⁴¹*AstroCeNT, Nicolaus Copernicus Astronomical Center, 00-614 Warsaw, Poland*
⁴²*Radiation Physics Laboratory, Belgorod National Research University, Belgorod 308007, Russia*
⁴³*Physics and Astronomy Department, University of California, Los Angeles, California 90095, USA*
⁴⁴*Department of Physics and Astronomy, University of Hawai'i, Honolulu, Hawaii 96822, USA*
⁴⁵*Université Paris-Saclay, CEA, List, Laboratoire National Henri Becquerel (LNE-LNHB), F-91120 Palaiseau, France*
⁴⁶*Chemistry, Biology and Biotechnology Department, Università degli Studi di Perugia, Perugia 06123, Italy*
⁴⁷*INFN Perugia, Perugia 06123, Italy*
⁴⁸*Department of Physics, University of California, Davis, California 95616, USA*
⁴⁹*M. Smoluchowski Institute of Physics, Jagiellonian University, 30-348 Krakow, Poland*
⁵⁰*The University of Manchester, Manchester M13 9PL, United Kingdom*



(Received 28 July 2022; accepted 6 January 2023; published 6 March 2023)

We present a search for dark matter particles with sub-GeV/ c^2 masses whose interactions have final state electrons using the DarkSide-50 experiment's ($12\,306 \pm 184$) kg d low-radioactivity liquid argon exposure. By analyzing the ionization signals, we exclude new parameter space for the dark matter-electron cross section $\bar{\sigma}_{e^*}$, the axioelectric coupling constant g_{Ae^*} , and the dark photon kinetic mixing parameter κ . We also set the first dark matter direct-detection constraints on the mixing angle $|U_{e4}|^2$ for keV/ c^2 sterile neutrinos.

DOI: [10.1103/PhysRevLett.130.101002](https://doi.org/10.1103/PhysRevLett.130.101002)

The very nature of dark matter (DM) remains unknown despite cosmological and astronomical observations collecting evidence of its existence over the last several decades [1–5]. Traditionally, DM particles with masses ranging from a GeV/ c^2 to few TeV/ c^2 have been extensively searched for by experiments located in underground laboratories by detecting their interactions with baryonic matter via elastic scattering off atomic nuclei [6–13]—usually called nuclear recoils (NRs). Heavy DM can also scatter off electrons, but the energy of such interactions—called electron recoils (ERs)—is suppressed due to the small electron mass. The lack of concrete evidence of direct DM detection motivates the search for other candidates and their possible interactions via scattering off, or absorption by, shell electrons, which may subsequently produce sufficiently large ionization signals in the detector [14].

This Letter reports on the analysis of the 653.1 live-days of data collected with the DarkSide-50 experiment (DS-50)

to probe DM interactions in the form of light DM-electron scattering, absorption of bosonic DM (axionlike particles and dark photons), and sterile neutrino-electron scattering. This analysis uses a more accurate calibration of the detector response [15], improved background modeling and determination of its systematic uncertainties [16], and a larger dataset compared to the previous study [17]. The same analysis approach was also applied to improve existing limits on spin-independent WIMP-nucleon interactions for WIMP masses down to 1.2 GeV/ c^2 [16] and down to 40 MeV/ c^2 when including the Migdal effect [18].

DS-50 is a dual-phase time projection chamber (TPC) housed in Italy's INFN Laboratori Nazionali del Gran Sasso (LNGS). The active volume consists of low-radioactivity underground liquid argon (LAr). Construction and performance details regarding the DS-50 detector are described in Ref. [19]. Two measurable signals can be observed: the light from scintillation in the liquid (S1) and ionization electrons, which are drifted using a 200 V/cm electric field in the LAr volume and extracted by a 2.8 kV/cm electric field into the gas phase, producing electroluminescence photons (S2) under acceleration by a 4.2 kV/cm electric field in the GAR volume. Two arrays of 19 3-in photomultiplier tubes (PMTs), one above the

Published by the American Physical Society under the terms of the [Creative Commons Attribution 4.0 International license](https://creativecommons.org/licenses/by/4.0/). Further distribution of this work must maintain attribution to the author(s) and the published article's title, journal citation, and DOI. Funded by SCOAP³.

anode and one below the cathode, detect photons. The DS-50 TPC, enclosed in a stainless steel double-walled, vacuum-insulated cryostat, lies inside a 30 t boron-loaded liquid scintillator veto instrumented by 110 8-in PMTs—to actively reject neutrons *in situ*—surrounded by a 1 kt water Cerenkov veto with 80 PMTs—to actively tag cosmic muons and act as a passive shield against external backgrounds.

The data selection criteria for this analysis aim to identify single-scatter, low-energy events in the form of paired S1 and S2 or S2-only pulses uncorrelated to any previous event. Various quality and selection cuts based on the ratio of S1 and S2, S2 signal time profile, and S2 distribution across the PMT arrays are implemented [16]. These cuts remove pileup pulses, surface α events inducing electrons from the cathode, and spurious trapped ionization electrons released up to 20 ms after the previous event. Moreover, only events reconstructed in the fiducial volume are selected, defined by the seven central top PMTs [16]. Veto detector signals are not used in the data selection since S2 triggers are delayed with respect to the veto by the electron drift time in the TPC. Figure 1 shows the final ionization spectrum obtained after all cuts described in [16], resulting in a fiducial mass of (19.4 ± 0.3) kg and exposure of $(12\,306 \pm 184)$ kg d.

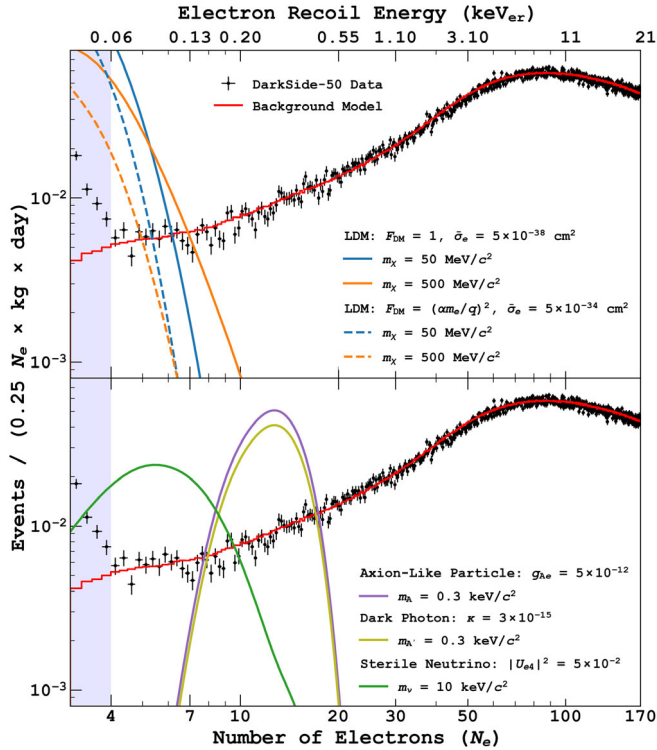


FIG. 1. Data (black) and background model (red) compared to expected ionization spectra of illustrative mass values for DM candidates: LDM heavy (blue and orange solid lines) and light (blue and orange dashed lines) mediators, ALPs (purple), dark photons (yellow), and sterile neutrinos (green). The region shaded blue is below threshold. Details on the background model and its fit can be found in Ref. [16].

This analysis is performed in the energy interval 4 to $170e^-$ (0.06 to 21 keV_{er}), up to the range of validity of the detector energy response calibration [16]. The low threshold is introduced to avoid the region dominated by spurious electrons.

The background model accounts for the natural radioactivity present in the LAr bulk due to ^{39}Ar and ^{85}Kr contamination, and γ 's and x rays from detector components like the PMT s, the TPC structure, and stainless-steel cryostat whose specific activities were determined via a comprehensive material screening campaign. For each, the ionization spectra with associated uncertainties were obtained via a detailed Monte Carlo simulation of DS-50 [16,20]. The red curve in Fig. 1 shows the background model fitted to data.

In this Letter, we search for several DM candidates using the DS-50 dataset and background model. The candidates are assumed to be nonrelativistic and comprise all of the galactic DM. While additional local sources for dark matter may be present (e.g., solar production of dark photons [21]), we set constraints using the interaction rates for the candidate only according to the standard halo model. Following the recommendations in Ref. [22], we assume a local DM density (ρ_{DM}) of 0.3 GeV/(c^2 cm 3), a standard isothermal Maxwellian velocity distribution ($f(v)$ where v the DM's velocity) with an escape velocity of 544 km/s, and a local standard of rest velocity of 238 km/s. Moreover, the predicted ionization rates per unit mass (R) are expressed as a function of the outgoing electron's recoil energy E_{er} . Using the argon ionization response, the spectra are expressed in number of electrons (N_e). The ionization response is obtained from the ^{39}Ar β -decay sample from an atmospheric argon campaign and from the low-energy ^{37}Ar peaks. ^{37}Ar was present in the first few months of DS-50 data and decayed away before the present dataset [15]. The detector response model [20] is applied to obtain the ionization spectra shown in Fig. 1.

Fermion or scalar boson light dark matter (LDM) candidates, with masses below a GeV/ c^2 , can interact with bound electrons via a vector mediator, resulting in the ionization of argon atoms. The LDM-electron interaction's dependence on the momentum-transfer q is encapsulated by a dark matter form factor $F_{\text{DM}}(q)$. The ionization rate for a LDM candidate of mass m_χ is parametrized by a reference cross section $\bar{\sigma}_e$ as [14,23,24]:

$$\frac{dR}{d\ln E_{\text{er}}} = N_T \frac{\rho_{\text{DM}}}{m_\chi} \times \frac{\bar{\sigma}_e}{8\mu_{\chi e}^2} \times \sum_{n\ell} \int |f_{\text{ion}}^{n\ell}(k', q)|^2 |F_{\text{DM}}(q)|^2 \eta(v_{\text{min}}) q dq, \quad (1)$$

where N_T is the number of target atoms per unit mass, $\mu_{\chi e}$ is the DM-electron reduced mass, $f_{\text{ion}}^{n\ell}(k', q)$ is the ionization form factor modeling the effects of the bound

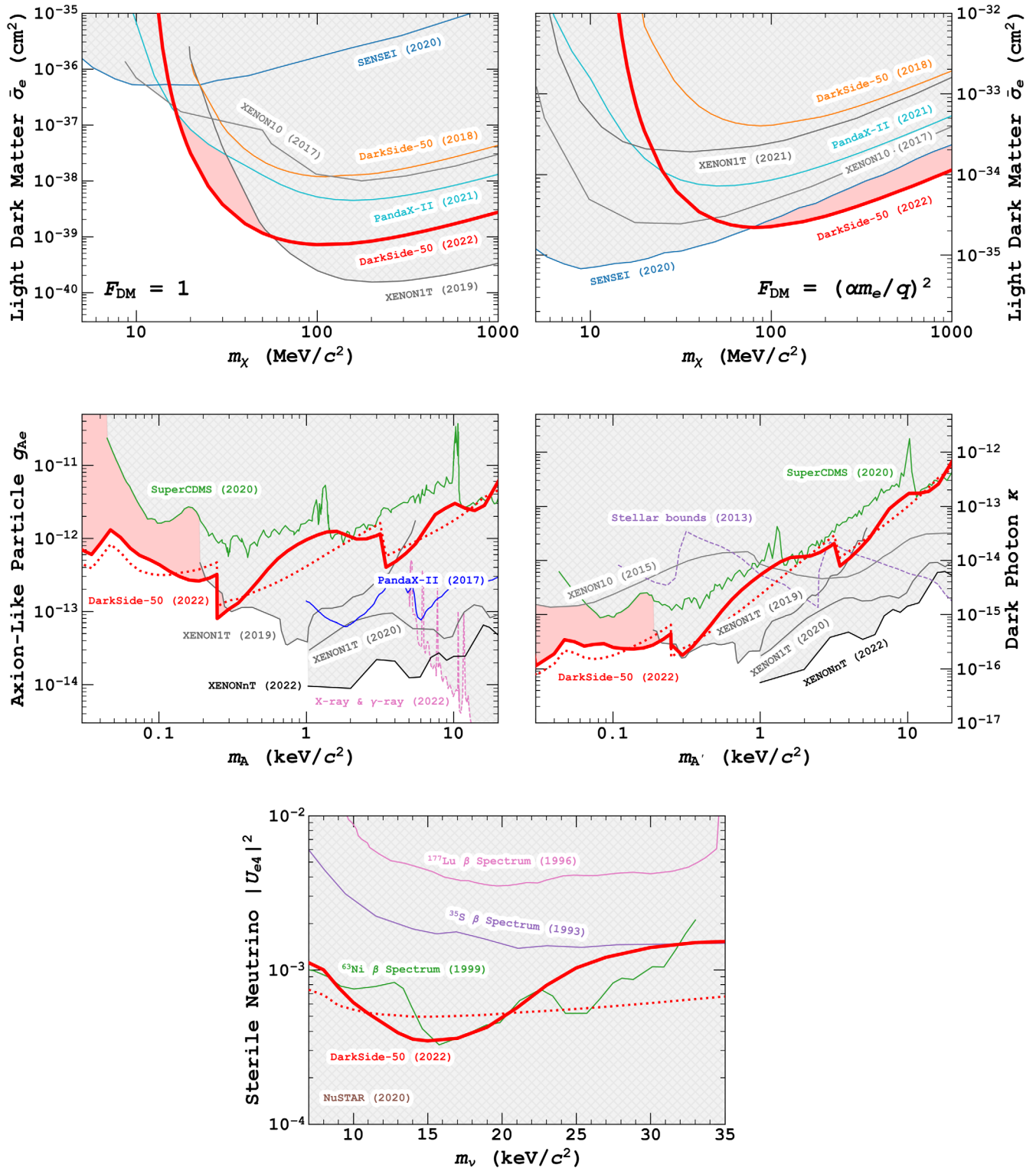


FIG. 2. Exclusion limits at 90% C.L. on DM particle interactions with electron final states. The x axis shows the mass of the candidate while the y axis shows the model parameter. Limits set by this work are shown as solid red lines while the -1σ expected limits are dotted red lines, and newly excluded parameter space is shaded red. Limits from laboratory experiments, shown as solid lines, are set by β spectrum analyses [36–38], DS-50 [23], PandaX-II [25,39], SENSEI [40], SuperCDMS Soudan [41], XENON10 [24,42], and XENON1T [43–45], with previously excluded parameter space shaded gray. Astrophysical constraints (dashed lines) are set by Refs. [46–49]. For sterile neutrinos, the limits set by NuSTAR [49] extend downwards to $|U_{e4}|^2 = 10^{-13}$ at 20 keV/c². All limits using the standard halo model are scaled to a local dark matter density ρ_{DM} of 0.3 GeV/(c² cm³).

electron in the (n, ℓ) shell and outgoing final state, $k' = \sqrt{2m_e E_{\text{er}}}$ is the electron recoil momentum, and $\eta(v_{\text{min}}) = \int (1/v)f(v)\Theta(v - v_{\text{min}})dv$ is the inverse mean speed function that encodes the DM velocity profile for the minimum DM velocity (v_{min}) required to eject an electron with E_{er} given q [23]. Two benchmark interaction models are considered: a heavy mediator (mass $\gg am_e$) with $F_{\text{DM}} = 1$ and a light mediator (mass $\ll am_e$) with $F_{\text{DM}} = (\alpha m_e/q)^2$, where α is the fine structure constant and m_e is the electron mass.

DS-50 is also sensitive to pseudoscalar DM such as axionlike particles (ALPs) [25–28] or vector-boson DM like dark photons [29] through absorption by argon shell electrons. Absorption of either candidate would result in a monoenergetic signal at the particle’s rest mass, m_A for an ALP or $m_{A'}$ for a dark photon. The absorption rate per unit mass of galactic ALPs depends on the axion-electron coupling strength g_{Ae} [28,29],

$$R = N_T \frac{\rho_{\text{DM}}}{m_A} \times \frac{3m_A^2 g_{Ae}^2}{16\pi\alpha m_e^2} \sigma_{\text{pe}}(m_A c^2), \quad (2)$$

while that of dark photons depends on the strength of the kinetic mixing κ between the photon and dark photon [29],

$$R = N_T \frac{\rho_{\text{DM}}}{m_{A'}} \times \kappa^2 \sigma_{\text{pe}}(m_{A'} c^2), \quad (3)$$

where σ_{pe} is argon’s photoelectric cross section [30] evaluated at the particle’s rest energy.

A sterile neutrino ν_s with a mass between 7 and 36 keV/ c^2 can be a viable DM candidate [31,32]. Sterile neutrinos interact via $\nu_s + e \rightarrow \nu_e + e$ (and $\bar{\nu}_s + e \rightarrow \bar{\nu}_e + e$) [33], where a ν_s mixing with an active state—parametrized by the mixing angle $|U_{e4}|^2$ —inelastically scatters off a bound electron in the detector. The ionization rate is governed by the cross section $\sigma_{n\ell}$ between ν_s and an electron in a given orbital (n, ℓ) [33]:

$$\frac{dR}{dE_{\text{er}}} = N_T \frac{\rho_{\text{DM}}}{m_\nu} \sum_{n\ell} 2(2\ell + 1) \int \frac{d\sigma_{n\ell}(v, m_\nu, |U_{e4}|^2)}{dE_{\text{er}}} f(v) v dv, \quad (4)$$

where m_ν is the sterile neutrino’s mass. We note that Eq. (4) does not include the effects of the ion on the outgoing electron, unlike the treatment of LDM-electron scattering in Eq. (1). Additionally, we note that the scattering rates calculated in Ref. [33] fail to evaluate the DM velocity distribution in the lab frame; however, this is corrected in our work.

This analysis employs a binned profile likelihood ratio (PLR) approach [34,35] to determine exclusion limits for each DM candidate. The PLR includes a set of nuisance parameters representing the nominal values and uncertainties on the exposure, materials screening,

theoretical energy spectra shape, and ionization energy scale. Correlations among the different components are encoded in the likelihood definition. See Ref. [16] for a complete description of the above. We also verified that the expected limits have negligible dependence on ER fluctuations by changing the Gaussian model described in Ref. [16] to a binomial one.

Figure 2 shows the 90% C.L. (Confidence Level) exclusion limits placed on each candidate via the PLR method. The observed limits (solid red lines) are shown alongside the expected limits at -1σ (dotted red lines) for ALPs, dark photons, and sterile neutrinos to show regions where observed limits are driven by underfluctuations of data.

We have established the best direct-detection limits on dark matter-electron scattering in the mass range of 16 to 56 MeV/ c^2 for a heavy mediator and above 80 MeV/ c^2 for a light mediator, with newly excluded parameter space shaded red. These new DS-50 results on LDM-electron scatters improve upon those previously obtained in 2018 [23] primarily due to the refined data selection criterion that suppresses correlated events between $4e^-$ and $7e^-$ [16]. Additional sensitivity gain comes from improved data selection, a more accurate detector calibration, improved background modeling, and a larger dataset.

We have also placed the first constraints on galactic axionlike particles and dark photons with an argon target. Stronger direct-detection limits are placed on both g_{Ae} and κ for masses between 0.03 and 0.2 keV/ c^2 .

DS-50 is the first DM direct-detection experiment to set limits on the sterile neutrino mixing angle $|U_{e4}|^2$. Under the standard halo model assumption, our results improve upon existing direct limits set by a high-precision measurement of the ^{63}Ni β spectrum [36]. However, these are well above the indirect detection limits set by the NuSTAR experiment [49], which looks for anomalous x-ray lines from radiative sterile neutrino DM decays.

The upcoming DarkSide-20k experiment has a planned exposure almost 4 orders of magnitude larger than DS-50 and will provide more sensitive searches for each DM model considered here.

The DarkSide Collaboration offers its profound gratitude to the LNGS and its staff for their invaluable technical and logistical support. We also thank the Fermilab Particle Physics, Scientific, and Core Computing Divisions. Construction and operation of the DarkSide-50 detector was supported by the U.S. National Science Foundation (NSF) (Grants No. PHY-0919363, No. PHY-1004072, No. PHY-1004054, No. PHY-1242585, No. PHY-1314483, No. PHY-1314501, No. PHY-1314507, No. PHY-1352795, No. PHY-1622415, and associated collaborative grants No. PHY-1211308 and No. PHY-1455351), the Italian Istituto Nazionale di Fisica Nucleare, the U.S. Department of Energy (Contracts No. DE-FG02-91ER40671, No. DEAC02-07CH11359, and No. DE-AC05-76RLO

1830), the Polish NCN (Grant No. UMO-2019/33/B/ST2/02884) and the Polish Ministry for Education and Science (Grant No. 6811/IA/SP/2018). We also acknowledge financial support from the French Institut National de Physique Nucléaire et de Physique des Particules (IN2P3), the IN2P3-COPIN consortium (Grant No. 20-152), and the UnivEarthS LabEx program (Grants No. ANR-10-LABX-0023 and No. ANR-18-IDEX-0001), from the São Paulo Research Foundation (FAPESP) (Grant No. 2016/09084-0), from the Interdisciplinary Scientific and Educational School of Moscow University “Fundamental and Applied Space Research,” from the Program of the Ministry of Education and Science of the Russian Federation for higher education establishments, Project No. FZWG-2020-0032 (2019-1569), from IRAP AstroCeNT funded by FNP from ERDF, and from the Science and Technology Facilities Council, United Kingdom. I. Albuquerque is partially supported by the Brazilian Research Council (CNPq). This project has received funding from the European Union’s Horizon 2020 research and innovation program under Grant Agreement No. 952480. Isotopes used in this research were supplied by the United States Department of Energy Office of Science by the Isotope Program in the Office of Nuclear Physics.

-
- [1] S. M. Faber and J. S. Gallagher, *Annu. Rev. Astron. Astrophys.* **17**, 135 (1979).
- [2] A. Refregier, *Annu. Rev. Astron. Astrophys.* **41**, 645 (2003).
- [3] D. Clowe, M. Bradač, A. H. Gonzalez, M. Markevitch, S. W. Randall, C. Jones, and D. Zaritsky, *Astrophys. J.* **648**, L109 (2006).
- [4] R. Thompson, R. Davé, and K. Nagamine, *Mon. Not. R. Astron. Soc.* **452**, 3030 (2015).
- [5] P. A. R. Ade *et al.* (Planck Collaboration), *Astron. Astrophys.* **594**, A13 (2016).
- [6] A. Tan *et al.* (PandaX-II Collaboration), *Phys. Rev. D* **93**, 122009 (2016).
- [7] E. Aprile *et al.* (XENON Collaboration), *Phys. Rev. Lett.* **121**, 111302 (2018).
- [8] D. S. Akerib *et al.* (LUX Collaboration), *Phys. Rev. Lett.* **118**, 021303 (2017).
- [9] P. Agnes *et al.* (DarkSide Collaboration), *Phys. Rev. D* **98**, 102006 (2018).
- [10] R. Ajaj *et al.* (DEAP Collaboration), *Phys. Rev. D* **100**, 022004 (2019).
- [11] R. Agnese *et al.* (SuperCDMS Collaboration), *Phys. Rev. Lett.* **112**, 041302 (2014).
- [12] H. Jiang *et al.* (CDEX Collaboration), *Phys. Rev. Lett.* **120**, 241301 (2018).
- [13] A. H. Abdelhameed, G. Angloher, P. Bauer, A. Bento, E. Bertoldo *et al.* (CRESST Collaboration), *Phys. Rev. D* **100**, 102002 (2019).
- [14] R. Essig, J. Mardon, and T. Volansky, *Phys. Rev. D* **85**, 076007 (2012).
- [15] P. Agnes *et al.* (DarkSide Collaboration), *Phys. Rev. D* **104**, 082005 (2021).
- [16] P. Agnes *et al.* (DarkSide-50 Collaboration), companion paper, *Phys. Rev. D* **107**, 063001 (2023).
- [17] P. Agnes *et al.* (DarkSide Collaboration), *Phys. Rev. Lett.* **121**, 081307 (2018).
- [18] P. Agnes *et al.* (DarkSide Collaboration), preceding Letter, *Phys. Rev. Lett.* **130**, 101001 (2023).
- [19] P. Agnes *et al.*, *Phys. Lett. B* **743**, 456 (2015).
- [20] P. Agnes *et al.*, *J. Instrum.* **12**, P10015 (2017).
- [21] I. M. Bloch, R. Essig, K. Tobioka, T. Volansky, and T.-T. Yu, *J. High Energy Phys.* **06** (2017) 087.
- [22] D. Baxter *et al.*, *Eur. Phys. J. C* **81**, 907 (2021).
- [23] P. Agnes *et al.* (DarkSide Collaboration), *Phys. Rev. Lett.* **121**, 111303 (2018).
- [24] R. Essig, T. Volansky, and T.-T. Yu (XENON Collaboration), *Phys. Rev. D* **96**, 043017 (2017).
- [25] C. Fu *et al.* (PandaX-II Collaboration), *Phys. Rev. Lett.* **119**, 181806 (2017).
- [26] E. Aprile *et al.* (XENON100 Collaboration), *Phys. Rev. D* **90**, 062009 (2014).
- [27] D. S. Akerib *et al.* (LUX Collaboration), *Phys. Rev. Lett.* **118**, 261301 (2017).
- [28] K. Arisaka, P. Beltrame, C. Ghag, J. Kaidi, K. Lung, A. Lyashenko, R. Peccei, P. Smith, and K. Ye, *Astropart. Phys.* **44**, 59 (2013).
- [29] M. Pospelov, A. Ritz, and M. Voloshin, *Phys. Rev. D* **78**, 115012 (2008).
- [30] B. Henke, E. Gullikson, and J. Davis, *At. Data Nucl. Data Tables* **54**, 181 (1993).
- [31] M. Leo, C. M. Baugh, B. Li, and S. Pascoli, *J. Cosmol. Astropart. Phys.* **11** (2017) 017.
- [32] A. Schneider, D. Anderhalden, A. V. Macciò, and J. Diemand, *Mon. Not. R. Astron. Soc.* **441**, L6 (2014).
- [33] M. D. Campos and W. Rodejohann, *Phys. Rev. D* **94**, 095010 (2016).
- [34] G. Cowan, K. Cranmer, E. Gross, and O. Vitells, *Eur. Phys. J. C* **71**, 1554 (2011).
- [35] L. Moneta, K. Cranmer, G. Schott, and W. Verkerke, *Proc. Sci.*, ACAT2010 (2011) 057.
- [36] E. Holzschuh, W. Kündig, L. Palermo, H. Stüssi, and P. Wenk, *Phys. Lett. B* **451**, 247 (1999).
- [37] J. L. Mortara, I. Ahmad, K. P. Coulter, S. J. Freedman, B. K. Fujikawa, J. P. Greene, J. P. Schiffer, W. H. Trzaska, and A. R. Zeuli, *Phys. Rev. Lett.* **70**, 394 (1993).
- [38] S. Schönert, L. Oberauer, C. Hagner, F. Feilitzsch, K. Schreckenbach, Y. Declais, and U. Mayerhofer, *Nucl. Phys. B, Proc. Suppl.* **48**, 201 (1996).
- [39] C. Cheng, X. Zhou, X. Chen, Y. Chen, X. Cui *et al.* (PandaX-II Collaboration), *Phys. Rev. Lett.* **126**, 211803 (2021).
- [40] L. Barak, I. M. Bloch, M. Cababie, G. Canelo, L. Chaplinsky *et al.* (SENSEI Collaboration), *Phys. Rev. Lett.* **125**, 171802 (2020).
- [41] T. Aralis *et al.*, *Phys. Rev. D* **101**, 052008 (2020).
- [42] H. An, M. Pospelov, J. Pradler, and A. Ritz, *Phys. Lett. B* **747**, 331 (2015).
- [43] E. Aprile *et al.* (XENON Collaboration), *Phys. Rev. Lett.* **123**, 251801 (2019).

- [44] E. Aprile *et al.* (XENON1T Collaboration), *Phys. Rev. D* **106**, 022001 (2022).
- [45] E. Aprile and others, *Phys. Rev. D* **102**, 072004 (2020).
- [46] N. Viaux, M. Catelan, P.B. Stetson, G.G. Raffelt, J. Redondo, A. A. R. Valcarce, and A. Weiss, *Phys. Rev. Lett.* **111**, 231301 (2013).
- [47] R. Z. Ferreira, M. C. D. Marsh, and E. Müller, *Phys. Rev. Lett.* **128**, 221302 (2022).
- [48] H. An, M. Pospelov, and J. Pradler, *Phys. Lett. B* **725**, 190 (2013).
- [49] B. M. Roach, K. C. Y. Ng, K. Perez, J. F. Beacom, S. Horiuchi, R. Krivonos, and D. R. Wik, *Phys. Rev. D* **101**, 103011 (2020).